Two-dimensional thermal illusion device with arbitrary shape based on complementary media*

Ge Xia(夏舸), Wei Kou(寇蔚), Li Yang(杨立)†, and Yong-Cheng Du(杜永成)

Department of Power Engineering, Naval University of Engineering, Wuhan 430033, *China*

(Received 11 April 2017; revised manuscript received 1 June 2017; published online 10 September 2017)

On the basis of transformation thermodynamics and compensation medium theory, we develop a method to design a two-dimensional thermal illusion device with arbitrary shape, and the general expression of thermal conductivity in the each region is obtained. Simulation results show that when an object is covered with the thermal illusion device, it will accurately perform the same temperature distribution signature as another object we have predetermined. Owing to the property of deceiving and interfering with the observer, the thermal illusion device can achieve generalized thermal stealth by using thermal metamaterials, which may have a potential application in military field.

Keywords: transformation thermodynamics, compensation medium, thermal illusion device, temperature distribution

PACS: 44.10.+I, 05.70.–a, 81.05.Xj, 07.05.Tp **DOI:** 10.1088/1674-1056/26/10/104403

1. Introduction

By analogy with the method of manipulating the flow of electromagnetic energy,[1,2] recently thermal metamaterials have been presented to control the path of heat fluxes based on the form-invariability of the heat diffusion equation. In 2008, Fan *et al.*[3] used a class of shaped graded material to design a spherical thermal cloak and spheroidal thermal cloak, and verified their performances through simulation. This is the first time that the transformation thermodynamic theory has been proposed and validated, and it was confirmed by Chen *et al.*[4] quickly. The previous studies mainly focused on the steady state thermal cloak, and Guenneau *et al.*[5] constructed a two-dimensional transient thermal cloak and concentrator by using 20-layer concentric homogeneous materials. In the same year, Narayana and Sato[6] designed a multilayer structure to control the direction of heat fluxes according to the equivalent medium theory, which can meet the requirements of engineering applications. On this basis, Schittny *et al.*[7] experimentally realized a transient thermal cloak by utilizing copper and PDMS. Recently, Mao *et al.*[8] and Xia *et al.*[9] derived the expressions for two-dimensional thermal cloak and three-dimensional thermal cloak with arbitrary shape respectively. The theory of transformation thermodynamics can be used to not only fabricate thermal cloak,[10–12] but also design different kinds of novel thermal devices, such as thermal concentrators,[13–15] thermal rotators,[16,17] heat flux converters,[18] thermal illusion devices,[19–21] and thermal camouflage devices,[22–24] and so on.

In the infrared stealth technology, the temperature difference between the target region and background region is used to identify the target. In this sense, if someone can use some methods to change the temperature distribution signature of object A to that of another object B we designed, the object A will appear to be like object B in the eyes of the observer. However, most of the illusion devices reported in the literature[19,21] are still limited to regular shapes, which are far from enough to meet the needs. The thermal illusion device proposed by He and Wu[20] was designed to have two regions with anisotropic thermal conductivity including the scope of the target, which is not possible in the infrared stealth technology. In this paper, according to the illusion optics proposed in Ref. [25] we design a thermal illusion device consisting of two distinct parts of metamaterials, which are called the "complementary region" and the "rebuilding region" respectively The complementary region is used to cancel the scatter of object while the rebuilding region can reconstruct the signature of another object we predetermined. According to transformation thermodynamics, the thermal conductivity expression in each of the two regions in the device is derived. The simulation results based on the finite element method confirm the function of this two-dimensional thermal illusion device for different objects with arbitrary shape and property In the end, we use homogeneous isotropic materials to construct the thermal device in light of the equivalent medium theory.

2. Theoretical model and design method

The heat conduction is that heat flux flows from the region of high temperature to the region of low temperature.[26] Here we start from the heat diffusion equation of steady state in the

*Project supported by the National Natural Science Foundation of China (Grant No. 11504426) and the National Defense Foundation of China (Grant No. 1010502020202).

†Corresponding author. E-mail: yangli123123@126.com

© 2017 Chinese Physical Society and IOP Publishing Ltd

cylindrical coordinates system without the heat source[27]

$$\nabla \cdot (\lambda \nabla T) = 0, \tag{1}$$

where λ is the thermal conductivity, T denotes the temperature of the point in the space, and ∇ represents the gradient operator.

According to the transformation thermodynamics theory, the transformed thermal conductivity λ' can be calculated from the following relationship[28]

$$\lambda' = \frac{\boldsymbol{A}\lambda\boldsymbol{A}^{\mathrm{T}}}{\det(\boldsymbol{A})}, \tag{2}$$

where $\boldsymbol{A}$ is the Jacobian transformation matrix which is determined by transform space and original space, λ' is the thermal conductivity in the transform space, and $\det(\boldsymbol{A})$ is the value of determinant $\boldsymbol{A}$.

The Jacobian matrix $\boldsymbol{A}$ in the cylindrical coordinate system[14] is

$$\boldsymbol{A} = \begin{bmatrix} \dfrac{\partial r'}{\partial r} & \dfrac{1}{r}\dfrac{\partial r'}{\partial \theta} & \dfrac{\partial r'}{\partial z} \\ r'\dfrac{\partial \theta'}{\partial r} & \dfrac{r'}{r}\dfrac{\partial \theta'}{\partial \theta} & r'\dfrac{\partial \theta'}{\partial z} \\ \dfrac{\partial z'}{\partial r} & \dfrac{1}{r}\dfrac{\partial z'}{\partial \theta} & \dfrac{\partial z'}{\partial z} \end{bmatrix}. \tag{3}$$

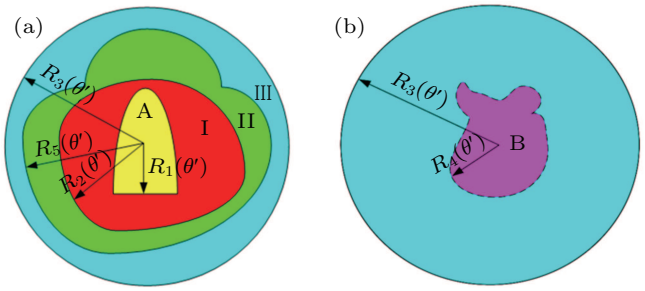


Fig. 1. (color online) Schematic diagram for overall structure of thermal illusion device.

Figure 1 shows the schematic for overall structure of thermal illusion device under our consideration. Specifically figure 1(a) illustrates that the object A is covered with an illusion device, while figure 1(b) displays that the object B is surrounded by the background. To create a thermal device shown in Fig. 1, we use two steps of spatial transformation similar to the designing of anti-cloak[29] First, the inner region of object A ($r' < R_1(\theta')$) is transformed into the region of complementary medium ($R_1(\theta') < r' < R_2(\theta')$), and the complementary region can cancel the thermal signature of object A. The corresponding coordinate transformation equation is

$$\begin{aligned} &r' = \frac{R_1 - R_2}{R_1} r + R_2, \quad \theta' = \theta, \quad z' = z, \\ &0 < r < R_1(\theta). \end{aligned} \tag{4}$$

Second, the rebuilt region is divided into two parts II ($R_2(\theta') < r' < R_5(\theta')$) and III ($R_5(\theta') < r' < R_3(\theta')$), and the coordinate transformation of this region is given as follows:

$$\begin{aligned} &r' = \frac{R_5 - R_2}{R_4} r + R_2, \\ &\theta' = \theta, \quad z' = z, \quad 0 < r < R_4(\theta), \end{aligned} \tag{5}$$

$$\begin{aligned} &r' = \frac{R_3 - R_5}{R_3 - R_4} r + \frac{R_5 - R_4}{R_3 - R_4} R_3, \\ &\theta' = \theta, \quad z' = z, \quad R_4(\theta) < r < R_3(\theta). \end{aligned} \tag{6}$$

The region with $0 < r < R_4(\theta)$ in the virtual space is folded into the region with $R_2(\theta') < r' < R_5(\theta')$ in the real space, while the region with $R_4(\theta) < r < R_3(\theta)$ in the virtual space is folded into the region with $R_5(\theta') < r' < R_3(\theta')$ in the real space.

According to Eqs. (4)–(6), we obtain the uniform coordinate transformation forms of the complementary region and the rebuilding region:

$$r' = m_i r + n_i, \quad i = 1,2,3, \quad \theta' = \theta, \quad z' = z, \tag{7}$$

where

$$\begin{aligned} m_1 &= \frac{R_1 - R_2}{R_1}, \quad n_1 = R_2, \\ m_2 &= \frac{R_5 - R_2}{R_4}, \quad n_2 = R_2, \\ m_3 &= \frac{R_3 - R_5}{R_3 - R_4}, \quad n_3 = \frac{R_5 - R_4}{R_3 - R_4} R_3. \end{aligned}$$

Substituting Eqs. (3) and (7) into Eq. (2), we can obtain the thermal conductivity λ' of the thermal illusion device in the cylindrical coordinate system:

$$\lambda'_{rr} = \frac{r' - n_i}{r'} \left[1 + \left(\frac{1}{m_i} \frac{\partial m_i}{\partial \theta'} + \frac{1}{r' - n_i} \frac{\partial n_i}{\partial \theta'} \right)^2 \right] \lambda_0, \tag{8a}$$

$$\lambda'_{r\theta} = \lambda'_{\theta r} = \left[\frac{1}{m_i} \frac{\partial m_i}{\partial \theta'} + \frac{1}{r' - n_i} \frac{\partial n_i}{\partial \theta'} \right] \lambda_0, \tag{8b}$$

$$\lambda'_{\theta\theta} = \frac{r'}{r' - n_i} \lambda_0, \tag{8c}$$

$$\lambda'_{zz} = \frac{r' - n_i}{m_i^2 r'} \lambda_0, \tag{8d}$$

$$\lambda'_{rz} = \lambda'_{zr} = \lambda'_{\theta z} = \lambda'_{z\theta} = 0, \tag{8e}$$

where λ_0 is the thermal conductivity in the virtual space.

The conversion relationship between the thermal conductivity in the Cartesian coordinate system and that in the cylindrical coordinates system is as follows:[12]

$$\lambda' = \begin{bmatrix} \cos\theta' & -\sin\theta' & 0 \\ \sin\theta' & \cos\theta' & 0 \\ 0 & 0 & 1 \end{bmatrix} \begin{bmatrix} \lambda'_{rr} & \lambda'_{r\theta} & \lambda'_{rz} \\ \lambda'_{\theta r} & \lambda'_{\theta\theta} & \lambda'_{\theta z} \\ \lambda'_{zr} & \lambda'_{z\theta} & \lambda'_{zz} \end{bmatrix} \times \begin{bmatrix} \cos\theta' & -\sin\theta' & 0 \\ \sin\theta' & \cos\theta' & 0 \\ 0 & 0 & 1 \end{bmatrix}^{\mathrm{T}}. \tag{9}$$

Substituting Eq. (8) into Eq. (9), the components of the thermal conductivity can be given in cylindrical coordinates as follows:

$$\lambda'_{xx} = \left[\frac{r'-n_i}{r'}\left(1+U^2\right)\cos^2\theta' - 2U\sin\theta'\cos\theta' + \frac{r'}{r'-n_i}sin^2\theta'\right]\lambda_0, \quad (10a)$$

$$\lambda'_{xy} = \lambda'_{yx} = \left\{\left[\frac{r'-n_i}{r'}\left(1+U^2\right) - \frac{r'}{r'-n_i}\right]\sin\theta'\cos\theta' + U(\cos^2\theta' - \sin^2\theta')\right\}\lambda_0, \quad (10b)$$

$$\lambda'_{yy} = \left[\frac{r'-n_i}{r'}\left(1+U^2\right)\sin^2\theta' + 2U\sin\theta'\cos\theta' + \frac{r'}{r'-n_i}\cos^2\theta'\right]\lambda_0, \quad (10c)$$

$$\lambda'_{zz} = \frac{r'-n_i}{m_i^2 r'}\lambda_0, \quad (10d)$$

where

$$U = \frac{1}{m_i}\frac{\partial m_i}{\partial\theta'} + \frac{1}{r'-n_i}\frac{\partial n_i}{\partial\theta'}.$$

3. Results and discussion

Finite element simulation is carried out to demonstrate the function of the designed thermal illusion device by utilizing the commercial software COMSOL Multiphysics. In the simulation, the parameters are set as follows: the outer radii of complementary region and rebuilding region are $R_2 = 2$ m and $R_3 = 4$ m respectively, the boundary between the rebuilding region II and region III is $R_5 = 3$ m. The whole region is a square area of 16 m×12 m, and the temperatures on the left and right side of region are set to be 400 K and 300 K, respectively. Both the bottom and top boundaries remain thermally insulated. Then, the heat fluxes flow from the left to the right. The background medium is set to be copper ($\lambda_0 =$ 400 W/(m·K)), the objects A and B are assumed to be stainless steel ($\lambda_1 = 15$ W/(m·K)) and silica gel ($\lambda_2 = 1.6$ W/(m·K)), respectively.

Figure 2 shows the results for the typical case when the objects A and B are both cylindrical. In this case, we set the radii of objects A and B are $R_1(\theta') = 1$ m and $R_4(\theta) = 2.5$ m, respectively. Figure 2(a) shows the temperature distribution when there is only a stainless steel object with radius 1 m embedded in the copper material. The grey solid lines represent the isothermal lines, showing that they curve inwards in the vicinity of the real object A. Comparing Fig. 2(b) with Fig. 2(c), it is clearly seen that the temperature distributions outside the thermal illusion device in the two pictures are the same. That is to say, when the observer watches targets from the left direction, he will take the object A made of stainless steel with a radius of 1 m for the object B made of silica gel with a radius of 2.5 m. To the observer, the thermal illusion device has perfect functions of confusion and disturbance.

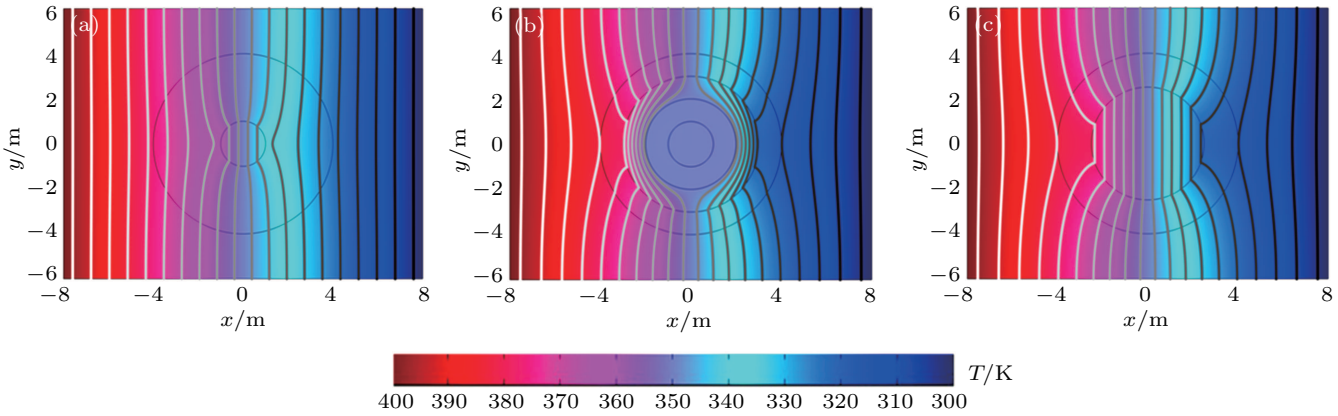


Fig. 2. (color online) Temperature profiles of (a) only round-shaped object A, (b) round-shaped object A with thermal illusion device and (c) only round-shaped object B.

To further verify the validity and generality of the derivation given in this paper, the simulation of a two-dimensional object with arbitrary shape covering thermal illusion device is carried out. In the simulation, the irregular outer boundaries of objects A and B are defined by the contour equations as follows:

$$R_1(\theta') = 1 + 0.1\sin\theta' - 0.1\sin 2\theta' + 0.2\cos 5\theta', \quad (11a)$$

$$R_4(\theta) = 2 + 0.2\sin\theta + 0.1\cos 2\theta + 0.2\sin 4\theta. \quad (11b)$$

Comparing Fig. 3(b) with Fig. 3(c), it is obvious that when a two-dimensional arbitrarily shaped object is covered with the designed thermal illusion device, and the temperature fields in the region of $r > R_3(\theta)$ are totally equivalent to the case when another object (predetermined) embedded in the same background. These results verify the effectiveness and correctness of the method of designing the thermal illusion device we proposed.

If thermal parameters of the virtual object B are the same as those of the background media, the device can achieve the effect of thermal stealth according to the above theory. The detailed simulation results are as follows.

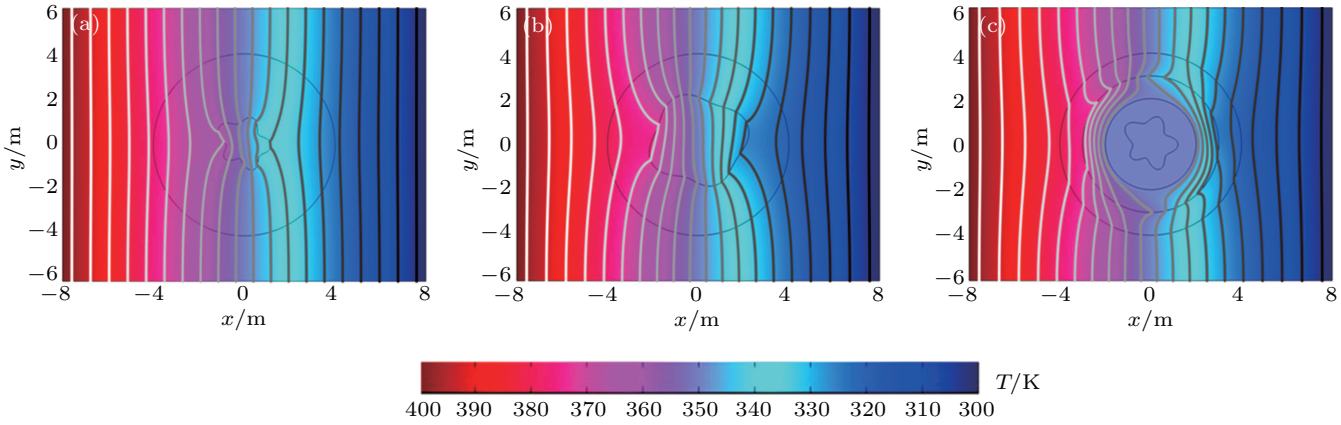


Fig. 3. (color online) Temperature profiles of (a) only object A in arbitrary shape, (b) in arbitrary shape with thermal illusion device, and (c) only object B in arbitrary shape.

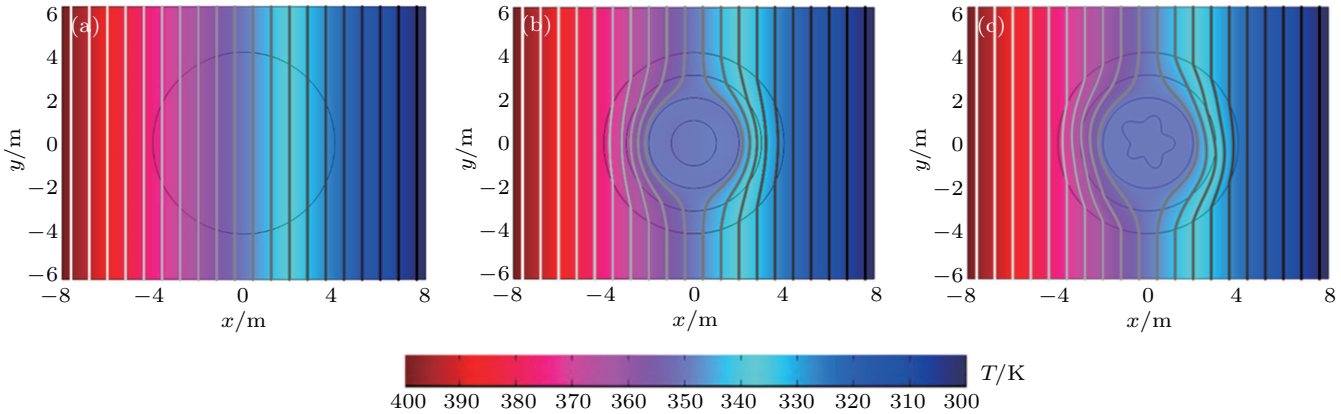


Fig. 4. (color online) Temperature distribution of (a) whole background, (b) round-shaped object with thermal illusion device, and (c) object in arbitrary shape with thermal illusion device.

Figure 4 shows the cloaking performances for thermal illusion devices covering the round shaped object and arbitrarily shaped object. It is obvious that regardless of the shape of the object A, the temperature distribution of the outer region $r > R_3(\theta)$ of the thermal illusion device is the same as that of the copper background. Unlike the traditional thermal cloaks designed in Refs. [13] and [28], this thermal illusion device has a typical feature that is the heat flux can flow into the cloaked object while keeping a perfect cloaking performance, which is consistent with the result of in Ref. [30]. That is to say, the object hidden inside the thermal illusion device has a feeling for the external heat flux.

According to the design method above, the device mainly consists of two parts, the complementary region I and the reconstructed regions II and III. As seen in Eqs. (8) and (10), the thermal conductivities of these thermal illusion devices should be not only anisotropic but also negative, which are difficult to achieve in nature. As a result, how to find proper materials to replace these metamaterials has become the focus of current research. In this work, we use three steps to homogenize the thermal conductivities of designed devices. As shown in Fig. 5(a), firstly, the entire device region with arbitrary shape is divided into M fan-shaped rings along the circumferential direction, and the inner and outer radii of those are estimated by the internal and external boundaries of the device. Thus, the thermal illusion device is approximated as the superposition of these fan-shaped rings. Secondly, each fan-shaped ring is divided into N layers in the radial direction, and the parameters of each layer are approximated by the central parameters. Lastly, each sub-layer can be approximated using two homogeneous isotropic media (An and Bn) as shown in Fig. 5(b). Assuming that the thickness values of the two materials A and B are equal, according to the effective medium theory,[31] it can be found that

$$\lambda_{\mathrm{A}} = \lambda'_{\theta\theta} + \sqrt{\lambda'_{\theta\theta}\left(\lambda'_{\theta\theta} - \lambda'_{rr}\right)}, \tag{12a}$$

$$\lambda_{\mathrm{B}} = \lambda'_{\theta\theta} - \sqrt{\lambda'_{\theta\theta}\left(\lambda'_{\theta\theta} - \lambda'_{rr}\right)}. \tag{12b}$$

Although the above method can be used to simplify the anisotropic material of the device into homogeneous isotropic materials, the medium in the complementary region is negative thermal conductivity material. It means that the heat flux in this region flows from low temperature to high temperature, which is contrary to the second law of thermodynamics we usually understood. By analogy with the working principle of an electric refrigerator, the negative thermal conductivity region can be achieved by external work.[19]

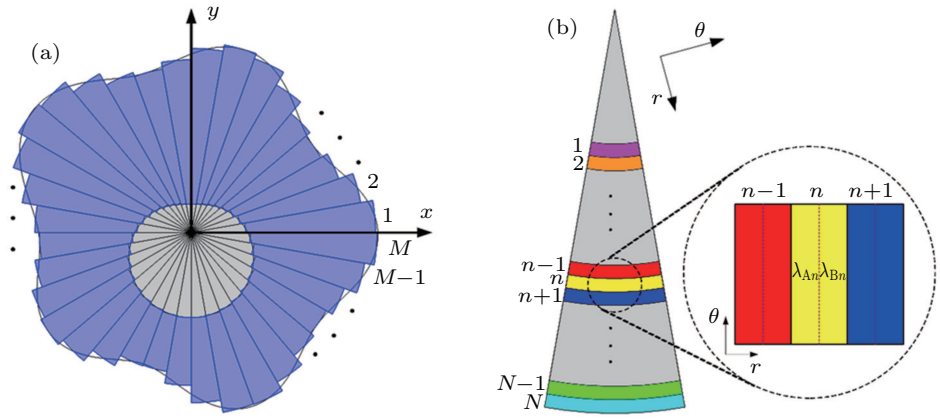


Fig. 5. (color online) Schematic diagram of stratification process for two-dimensional region with arbitrary shape: (a) the device divided into M fan-shaped rings along the circumferential direction; (b) the fan-shaped ring divided into N-layer subring along the radial direction, and each fan-shaped subring divided into two-layer alternative structure of homogeneous isotropic layers A and B.

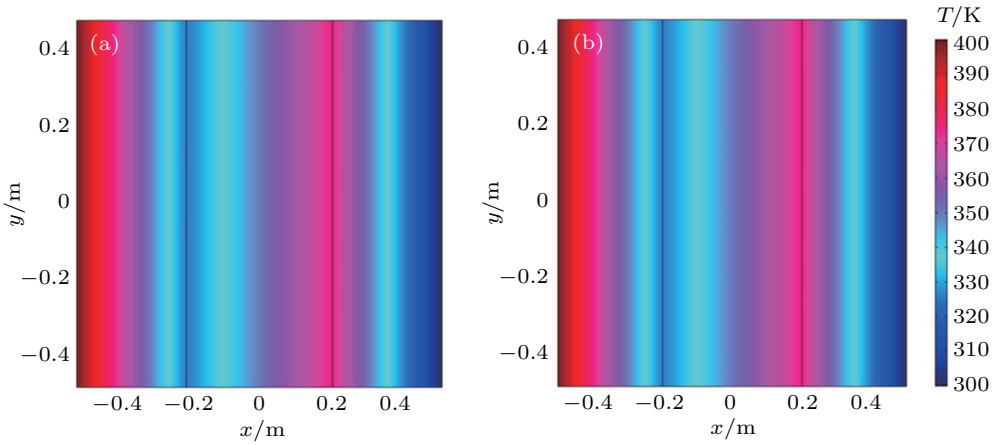


Fig. 6. (color online) (a) Temperature distributions for the cases with (a) negative values of thermal conductivities and (b) effective negative values of thermal conductivities, respectively.

As shown in Fig. 6, the size of whole simulation region is 1 m×1 m, and the left and right side of that are set to be 400 K and 300 K, respectively. Figure 6(a) shows the temperature distribution of a square region (0.4 m×1 m) with a negative thermal conductivity of −100 W/(m·K) embedded in the background region with a thermal conductivity of 50 W/(m·K). In Fig. 6(b), we replace the negative thermal conductivity with a thermal conductivity of 100 W/(m·K), and maintain the temperatures 325 K and 375 K respectively at $x = -0.2$ m and 0.2 m by external work. The exact values of the temperatures on the boundaries can be figured out by considering the continuity conditions and boundary conditions:

$$-\lambda_{\text{background}}\frac{\partial T}{\partial x}|_{x=\pm 0.2\text{ m}} = -\lambda_{\text{negative}}\frac{\partial T}{\partial x}|_{x=\pm 0.2\text{ m}},$$
$$T|_{x=-0.5\text{ m}} = 400\text{ K}, \quad T|_{x=0.5\text{m}} = 300\text{ K}.$$

The temperature distributions of two figures are exactly the same, which means that we can achieve the same effect as negative thermal conductivity by the above method.

4. Conclusions

In this paper, we propose a method of designing a special thermal illusion device to conceal the object with arbitrary shape. The thermal conductivities of the illusion device within all the subregions are deduced based on the transformation thermodynamics and equivalent medium theory. According to the conductivities, we design different kinds of devices, such as cylindrical thermal illusion devices, arbitrarily shaped devices and thermal anti-cloaks. We verify this method by the finite element software Comsol Multiphysics. The thermal illusion device can make the object just look like other totally different object (in the aspect of the temperature outside the device). Owing to this property, the object covered with this kind of thermal illusion device can confuse the detectors of opponent, which will have a great potential application in the military camouflage.

References

[1] Pendry J B, Schurig D and Smith D R 2006 *Science* **312** 1780
[2] Pendry J B, Schurig D and Smith D R 2006 *Opt. Express* **14** 9794
[3] Fan C Z, Gao Y and Huang J P 2008 *Appl. Phys. Lett.* **92** 251907
[4] Chen T Y, Weng C N and Chen J S 2008 *Appl. Phys. Lett.* **93** 114103
[5] Guenneau S, Amra C and Veynante D 2012 *Opt. Express* **20** 8207
[6] Narayana S and Sato Y 2012 *Phys. Rev. Lett.* **108** 214303
[7] Schittny R, Kadic M, Guenneau S and Wegener M 2013 *Phys. Rev. Lett.* **110** 195901
[8] Mao F C, Li T H, Huang M, Yang J J and Chen J C 2014 *Acta Phys. Sin.* **63** 014401 (in Chinese)

[9] Xia G, Yang L, Kou W and Du Y C 2017 *Acta Phys. Sin.* **66** 104401 (in Chinese)
[10] Yang T Z, Vemuri K P and Bandaru P R 2014 *Appl. Phys. Lett.* **105** 083908
[11] Yang T Z, Wu Q H, Xu W K, Liu D, Huang L J and Chen F 2016 *Phys. Lett. A* **380** 965
[12] Xia G, Yang L, Kou W and Du Y C 2017 *Acta Phys. Sin.* **66** 114401 (in Chinese)
[13] Shen X Y, Li Y, Jiang C R, Ni Y S and Huang J P 2016 *Appl. Phys. Lett.* **109** 031907
[14] Guenneau S, Amra C and Veynante D 2012 *Opt. Express* **20** 8207
[15] Peralta I, Fachinotti V D and Ciarbonetti Á A 2017 *Sci. Rep.* **7** 40591
[16] Guenneau S and Amra C 2013 *Opt. Express* **21** 6578
[17] Kadic M, Bückmann T, Schittny R and Wegener M 2013 *Rep. Prog. Phys.* **76** 126501
[18] Dede E M, Nomura T, Schmalenberg P and Lee J S 2013 *Appl. Phys. Lett.* **103** 063501
[19] Chen Y X, Shen X Y and Huang J P 2015 *Eur. Phys. J. Appl. Phys.* **70** 20901
[20] He X and Wu L Z 2014 *Appl. Phys. Lett.* **105** 221904
[21] Shen X Y, Chen Y X and Huang J P 2016 *Commun. Theor. Phys.* **65** 375
[22] Han T C, Bai X, Thong J T L, Li B W and Qiu C W 2014 *Adv. Mater.* **26** 1731
[23] Yang T Z, Bai X, Gao D L, Wu L Z, Li B W, Thong J T L and Qiu C W 2015 *Adv. Mater.* **27** 7752
[24] Yang T Z, Su Y, Xu W K and Yang X D 2016 *Appl. Phys. Lett.* **109** 121905
[25] Lai Y, Chen H Y, Zhang Z Q and Chan C T 2009 *Phys. Rev. Lett.* **102** 093901
[26] Rohsenow W M 1985 *Handbook of heat transfer fundamentals* (Los Angeles: McGraw-Hill Education) pp. 1–2
[27] Holman J P 2011 *Heat Transfer*, 10th edn. (Singapore: McGraw-Hill Education) pp. 2–5
[28] Yang T Z, Huang L J, Chen F and Xu W K 2013 *J. Phys. D: Appl. Phys.* **46** 305102
[29] Li L, Huo F F, Zhang Y M, Chen Y and Liang C H 2013 *Opt. Express* **21** 9422
[30] Shen X Y and Huang J P 2014 *Int. J. Heat Mass Transfer* **78** 1
[31] Yuan X B, Lin G C and Wang Y S 2016 *Mod. Phys. Lett. B* **30** 1650256